Theoretical Studies of a Highly Reactive Diacetylene Monomer, 3,5-Octadiyn-2,7-dione, and Its Cross-Conjugated PDA Oligomers

S. E. Zutaut and S. P. McManus*

Department of Chemistry, The University of Alabama in Huntsville, Huntsville, Alabama 35899

M. Jalali-Heravi

Chemistry Department, Shahid Bahonar University of Kerman, Kerman 76169, Iran

Received September 26, 1995. Revised Manuscript Received February 8, 1996[⊗]

Polydiacetylene derivatives have great potential in the area of nonlinear optics. Several factors affect the usefulness of these materials, and it is desirable to model the effects of these factors before time and resources are spent in the development of new materials. Our work focuses on a particular derivative, 3,5-octadiyn-2,7-dione, ODDO, which related work has shown to be highly polymerizable in solution. The interesting polymer poly-ODDO has acetyl groups cross-conjugated with the conjugated backbone. Calculations show that the monomer's reactivity may be partially explained on thermodynamic grounds. The utility of the AM1 method in MOPAC 6.0 as a model for PDA experimental optical properties is shown. Conformers of ODDO and its oligomers are calculated at high precision using AM1 to see the variation in optical properties and stability as a function of backbone planarity and substituent alignment relative to the backbone, in an effort to determine whether or not there would be any benefit in optical properties to attempts to control the conformation. Analysis of the data indicates that backbone planarity should be important to optical properties, as one would expect, and that substituent orientation has much less effect than one might expect from a cross-conjugated substituent. Specific coplanar orientations are predicted to have a large relative effect on stability but only a minor effect on optical properties. Coplanar ODDO oligomers are predicted to have lower HOMO−LUMO gaps and better third-order nonlinear optical properties than equivalent unsubstituted oligomers. The data also show that monomeric HOMO−LUMO gaps may not reliably predict the relative utility of polymeric nonlinear optical materials.

Introduction

Polydiacetylene (PDA) derivatives are organic polymers with π-conjugated backbones that exhibit interesting and potentially useful properties, including their large nonresonant second-order hyperpolarizabilities, γ, and their ability to undergo solid-state topochemical polymerization.[1] These phenomena have led us to study the use of semiempirical self-consistent field molecular orbital (SCF-MO) methods in modeling the geometries, electronic properties, and optical properties of PDA derivatives.[2−6]

There are two goals of this paper. The first goal is to show that semiempirical methods are useful in modeling nonlinear optical (NLO) properties of organic polymers, specifically PDA and its derivatives, by reproducing trends that have been observed experimentally. This is a continuation of previous theoretical and experimental work by our group that has shown the utility of such methods in modeling of the structure, stability, electronic properties, and topochemical polymerization of the monomeric diacetylene (DA) and its derivatives, and the structure and electronic properties of PDA and its derivatives.[2−6] The polymerization of diacetylene (DA) derivatives to polydiacetylene (PDA) derivatives is shown in Scheme 1.

The second goal of this paper is to apply those semiempirical methods to the analysis of a derivative of DA, the diketone 3,5-octadiyn-2,7-dione (ODDO), and its polymeric form, poly-ODDO, shown in Scheme 2. The

[⊗] Abstract published in *Advance ACS Abstracts,* July 15, 1996.

(1) General NLO references: (a) Zyss, J., Ed. *Molecular Nonlinear Optics*; Academic Press: San Diego, 1994. (b) Salomone, J. C., Ed. *Contemporary Topics in Polymer Science*; Plenum: New York, 1992; Vol. 7. (c) Prasad, P. N.; Williams, D. J. *Introduction to Nonlinear Optical Effects in Molecules and Polymers*; John Wiley & Sons, Inc.: New York, 1991. (d) Marder, S. R., Sohn, J. E., Stucky, G. D., Eds. *Materials for Nonlinear Optics: Chemical Perspectives*; American Chemical Society: Washington, DC, 1991. (e) André, J.; Delhalle, J. *Chem. Rev.* **1991**, *91*, 843. (f) Prasad, N. P., Ulrich, D. R., Eds. *Nonlinear Optical and Electroactive Polymers*; Plenum Press: New York, 1988. (g) Meridith, G. R. *MRS Bull.* **1988**, *13*(8), 24. (h) Heeger, A. J.; Ulrich, D. R. *Nonlinear Optical Properties of Polymers*; North-Holland Press: New York, 1988. (i) Prasad, P. N.; Ulrich, D. A. *Nonlinear Optical and Electroactive Polymers*; Plenum: New York, 1988. In-depth NLO references: (j) Newell, A. C.; Moloney, J. V. *Nonlinear Optics*; Addison-Wesley Publishing: New York, 1992. (k) Butcher, P. N.; Cotter, D. *The Elements of Nonlinear Optics*; Cambridge University Press: Cambridge, 1990. (l) Shen, Y. R. *The Principles of Nonlinear Optics*; John Wiley and Sons, Inc.: New York, 1984.

(2) McManus, S. P.; Patel, D. N.; McDonald, J. K. *Prepr. First Polym. Conf. (Pacific Polymer Federation)* **1989**, *1*, 207.

(3) Jalali-Heravi, M.; McManus, S. P.; Zutaut, S. E.; McDonald, J. K. *Macromolecules* **1991**, *24*, 1055.

(4) Jalali-Heravi, M.; Zutaut, S. E.; McManus, S. P. *Polym. Prepr.* **1991**, *32(1)*, 78.

(5) Zutaut, S. E.; Jalali-Heravi, M.; McManus, S. P. In ref 1b, pp 161−170.

(6) Paley, M. S.; Frazier, D. O.; Abeledeyem, H.; McManus, S. P.; Zutaut, S. E. *J. Am. Chem. Soc.* **1992**, *114*, 3247.

S0897-4756(95)00451-0 CCC: $12.00

Scheme 1

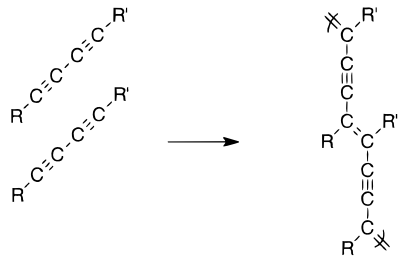

Diacetylene (DA) Derivative — Polydiacetylene (PDA) Derivative

Scheme 2

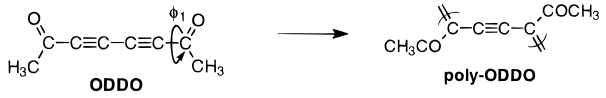

ODDO — poly-ODDO

selection of ODDO for theoretical study was prompted by an inability to isolate the monomer. Ongoing experimental work by our group has shown that ODDO oligomerizes when any attempt is made to concentrate it, indicating that this DA derivative is very reactive.[7] A possible reason for the monomer's reactivity could be its destabilization by the acetyl groups or the stabilization of reactive intermediates or the polymer by those conjugated pendant groups. Also, since poly-ODDO is a cross-conjugated polymer, it serves as a model for the theoretical analysis of the effects of cross-conjugation on the electronic and optical properties of PDA derivatives.

NLO Properties

As mentioned above, one of the goals of the research presented in this paper was to determine the usefulness of semiempirical methods in the prediction of NLO properties. The following is a brief discussion of the theory behind NLO properties.

The existence of NLO phenomena is represented at the microscopic level as a Taylor's expansion of the relationship between the spatial components of the induced dipole moment μ_i and the components of the electric field E_i that create it, as shown in eq 1, where

$$\mu_i = \mu_i^0 + \sum_j \alpha_{ij} E_j + {}^1/_2 \sum_{jk} \beta_{ijk} E_j E_k + {}^1/_6 \sum_{jkl} \gamma_{ijkl} E_j E_k E_l + \ldots \quad (1)$$

$\alpha_{ij} = (\partial \mu_i / \partial E_j)_{E0}$, $\beta_{ijk} = (\partial \mu_i / \partial E_j\, \partial E_k)_{E0}$ and $\gamma_{ijkl} = (\partial \mu_i / \partial E_j\, \partial E_k\, \partial E_l)_{E0}$. These tensors can also be developed from a Taylor's expansion of the Stark energy, as shown in eq 2, where $U(0)$ is the energy in the absence of the electric

$$U(\mathbf{E}) = U(0) - \sum_i \mu_i E_i - {}^1/_2 \sum_{ij} \alpha_{ij} E_i E_j - {}^1/_6 \sum_{ijk} \beta_{ijk} E_i E_j E_k - {}^1/_{24} \sum_{ijkl} \gamma_{ijkl} E_i E_j E_k E_l - \ldots \quad (2)$$

field $\mathbf{E}$, $\mu_i = (\partial U_i / \partial E_i)_{U0}$, $\alpha_{ij} = (\partial U_i / \partial E_i\, \partial E_j)_{U0}$, $\beta_{ijk} = (\partial U_i / \partial E_i\, \partial E_j\, \partial E_k)_{U0}$, and $\gamma_{ijkl} = (\partial U_i / \partial E_i\, \partial E_j\, \partial E_k\, \partial E_l)_{U0}$. Note that these approximations are valid only for fields and polarizations that are small relative to atomic fields. When small electric fields are employed, the terms containing β and γ components can be ignored and the relation is assumed to be linear.

The macroscopic equivalent of eqs 1 and 2 is shown in eq 3, which represents the relationship between the

$$P_i = \sum_j \chi_{ij}^{(1)} E_j + \sum_{jk} \chi_{ijk}^{(2)} E_j E_k + \sum_{jkl} \chi_{ijkl}^{(3)} E_j E_k E_l + \ldots \quad (3)$$

ith component of the polarization and the components of the incident field.

The χ terms are the first-order, second-order and third-order susceptibility tensors, respectively. These bulk quantities are the values that tend to be measured experimentally. However, the values that are usually calculated are the molecular quantities: α, β, and γ, which are the polarizability, first-order hyperpolarizability, and the second-order hyperpolarizability tensors, respectively. The relationship between respective quantities depends on molecular orientation and local electric field factors, and in some cases other effects such as intermolecular charge transfer.[1c] Unfortunately, the geometry of a molecule in the gas phase (the way they are usually calculated), solution, and solid state (the way they are employed in devices) can be quite different. The differences are a result of intermolecular interactions between molecules.

Cross-conjugation occurs when an electric field component along one axis can cause a polarization along another axis. This does not occur to a significant degree in many PDA derivatives, which are essentially one-dimensional, and therefore have only one significant γ component, assuming that the field is aligned along the axis of conjugation. This axis is represented as the x axis in this paper, and the significant second hyperpolarizability axial component is therefore γ_{xxxx}. The cross-conjugation terms are represented by the components in which the indexes are not the same. For example, a field along the x axis which causes a polarization change along the y axis would be represented by several components which are equivalent to γ_{xxyy}.

A value that is useful in measuring third-order NLO properties is the mean second hyperpolarizability $\langle\gamma\rangle$, which is calculated as shown in eq 4. This value is useful because it is independent of the frame of reference in which measurements are made.

$$\langle\gamma\rangle = {}^1/_5(\gamma_{xxxx} + \gamma_{yyyy} + \gamma_{zzzz} + 2(\gamma_{xxyy} + \gamma_{xxzz} + \gamma_{yyzz})) \quad (4)$$

Methods of Calculating NLO Properties. There are two major ways of calculating NLO properties: finite field methods,[8] which are utilized in the current work, and sum-over-state methods.[9,10] Both methods are now being used to calculate third-order NLO properties.

Finite-field methods are based on eqs 1 and/or 2 and involve using the definitions of the microscopic hyper-

(7) McManus, S. P.; Paley, M. S.; Somani, S., unpublished results.

(8) Kurtz, H. A.; Stewart, J. J. P.; Dieter, K. M. *J. Comput. Chem.* **1990**, *11*, 82.

(9) Heflin, J. R.; Garito, A. F. In *Electroresponsive Molecular and Polymeric Systems*; Skotheim, T. A., Ed.; Marcel Dekker, Inc.: New York, 1991; Vol. 2.

(10) Karna, S. P.; Dupuis, M. *J. Comput. Chem.* **1991**, *12*, 487.

polarizabilities as being numerical derivatives of either the dipole moment or the energy in the presence of a perturbing field. Alternatively, the values can be determined analytically as a function of the perturbed dipoles or energies as a function of the fields. In the case of γ, the components can be computed by using a series of different field strengths that are simple multiples of one another, and solving for the components in terms of them. This manipulation of eq 1 leads to the eqs 5 and 6. Alternatively, manipulation of eq 2 leads to eqs 7 and 8. To actually find the effect of a field on the system ($\mu(\mathbf{E})$ and $U(\mathbf{E})$), it is necessary to modify the Hamiltonian by including terms for field−electron interactions and sometimes field−nucleus interactions.

$$\gamma_{iiii}E_i^3 = {}^1/_2\mu_i(2E_i) - {}^1/_2\mu_i(-2E_i) + \mu_i(E_i) - \mu_i(-E_i) \quad (5)$$

$$\gamma_{iijj}E_iE_j^2 = {}^1/_2\mu_i(E_i,E_j) - {}^1/_2\mu_i(-E_i,E_j) + {}^1/_2\mu_i(E_i,-E_j) - {}^1/_2\mu_i(-E_i,-E_j) - \mu_i(E_i) - \mu_i(-E_i) \quad (6)$$

$$\gamma_{iiii}E_i^4 = -6U(0) + 4U(E_i) + 4U(-E_i) - U(2E_i) - U(-2E_i) \quad (7)$$

$$\gamma_{iijj}E_i^2E_j^2 = -4U(0) - U(E_i,E_j) - U(-E_i,-E_j) - U(E_i,-E_j) - U(-E_i,E_j) + 2U(E_i) + 2U(-E_i) + 2U(E_j) + 2U(-E_j) \quad (8)$$

Programs that use the sum-over-states approach for calculating third-order properties have also appeared within the past few years.[9,10] They calculate α, β, and γ as functions of the frequency of light, whereas finite-field methods generally assume zero frequency. This is desirable, particularly when it is important to know about effects near resonant frequencies, but usually requires more costly calculations which might make it unsuitable for calculating γ for large systems such as polymers.

Methods

Previous calculations[3] have indicated that one of the most promising semiempirical SCF-MO methods for predicting PDA derivative geometries and selected electronic properties is AM1 (Austin method 1),[11] as implemented in MOPAC.[12] Trends are consistent with experimental results, though specific values are not reproduced, e.g., the HOMO−LUMO gap. PM3 (parametric method 3)[13] is also useful, while the MNDO (modified neglect of differential orbitals)[14] method has been found to be unacceptable.

The more recent versions of MOPAC have routines which calculate optical properties,[11] including the mean second-order hyperpolarizability, $\langle\gamma\rangle$. MOPAC 6.0 was used exclusively for the work presented herein. The VAX version was ported to PC and compiled using Microway NDP FORTRAN-486.[15] All of the calculations presented by the authors were carried out on a Gateway 2000 P5-90 computer.

All calculations were performed using AM1 at high precision, using the keywords GNORM=0.D0 (equivalent to GNORM=0.01) and SCFCRT=1.D-15. The Eigenvector Following minimization routines were used in all cases, with the keywords EF and DMAX=0.05.

For the results presented in Figures 1−10, symmetry was used to enforce equivalent angles in the backbones. Symmetry was also imposed on the poly-ODDO models for both planar and nonplanar calculations, to impose equivalent backbone angles and geometries for equivalent substituents.

Calculations regarding optical properties were performed based on a finite-field method, which is frequency independent, using the POLAR keyword.[8] The values reported are all energy values, based on eqs 2, 7, and 8, which tend to have greater numerical stability than dipole moment values. There was little difference between the two sets of numbers in most cases (less than 2% difference).

For the oligomeric thermodynamic calculations, the keywords ROT=2, FORCE, and THERMO(298,298) were used. These keywords cause optimization of all geometric parameters, so no intramolecular symmetry relations could be defined. Note also that ROT=2 assumed an idealized geometry, which may not have been valid in some cases. Some runs were checked using ROT=1 for the less symmetric cases, and the deviations were found not to be of qualitative significance. Also, the thermodynamic calculations in MOPAC use the rigid-rotor assumption, which is not valid for some of the PDA derivatives. However, the effect of the flexibility should also be qualitatively insignificant at standard temperature (298 K) because it should be below the noise level introduced by the fact that vibrational frequencies derived from MO theory are being used to determine the thermodynamic quantities.[16] Note that only the differences in equivalent conformers (i.e., comparing monomers and monomeric units) should be compared in order to cancel systematic errors in the thermodynamic calculations.

Excited-state calculations were performed using the keywords for the optical properties, excluding POLAR, with the addition of the EXCITED keyword. All derivatives were completely minimized with the exception of the ditosylate, which because of its size was stopped after minimizing to a gradient norm of less than 0.2.

Results and Discussion

Viability of AM1 Optical Calculations. Despite the fact that polymers of DA derivatives, as well as most conjugated polymers, tend to be insoluble, making it very difficult to experimentally measure $\langle\gamma\rangle$ in solution, some data exist. Craig and co-workers[17] have carried out studies on triblock copolymers containing unsubstituted polyacetylene (another π-conjugated polymer with interesting NLO properties) as the middle polymer. For different numbers of polyacetylenic subunits, the

(11) Dewar, M. J. S.; Zoebisch, E. G.; Healy, E. F.; Stewart, J. J. P. *J. Am. Chem. Soc.* **1985**, *107*, 3902.
(12) Stewart, J. J. P. MOPAC, A Semiempirical Molecular Orbital Program, QCPE 455, 1983; Version 6.0; 1990.
(13) Stewart, J. J. P. *J. Comput. Chem.* **1989**, *10*, 221.
(14) Dewar, M. J. S.; Thiel, W. *J. Am. Chem. Soc.* **1977**, *99*, 4899, 4970.
(15) NDP Fortran-486, Version 4.2.0; Microway, Research Park, Box 79, Kingston, MA 02364; 992.
(16) Dewar, M. J. S.; Ford, G. P. *J. Am. Chem. Soc.* **1977**, *99*, 7822.
(17) Craig, G. S. W.; Cohen, R. E.; Schrock, R. R.; Silbey, R. J.; Puccetti; G.; Ledoux, I.; Zyss, J. *J. Am. Chem. Soc.* **1993**, *115*, 860.

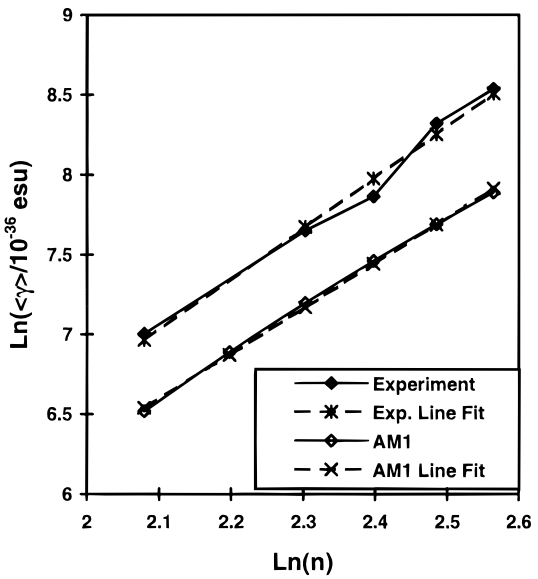

Figure 1. Plot of $\ln(\langle\gamma\rangle/10^{-36}$ esu) vs $\ln(n)$ for experiment $\langle\gamma\rangle$ values of acetylene oligomers and the best fit line, with slope $p = 3.1$; and AM1 calculated $\langle\gamma\rangle$ values of the same oligomers with the best fit line, with slope $p = 2.8$.

values for $\langle\gamma\rangle$ were measured as a function of the number of oligomer units. In that work, the data were plotted under the assumption that the relationship should be a simple power relation: $\langle\gamma\rangle = An^p$, based on various theories, which predict different numbers for p, ranging from 3 to 5.4. A plot of the experimental data indicates that p should be 3.1 for the all-trans conformer of polyacetylene, as shown in Figure 1. Now, let us consider the values for γ of polyacetylene oligomers that have been previously calculated by Kurtz using the AM1 method in MOPAC 6.0.[18] By plotting $\ln(\langle\gamma\rangle)$ vs $\ln(n)$, we would expect to see a linear relationship, with p as the slope. In fact, this is not what is seen. By selecting the same region that was used to determine the value of p in the experimental work (8−13 repeat units, excluding 9), the value calculated by drawing the best data through the points gives $p = 2.8$. This is a good agreement between the two sets of γ values. However, the value of p decreases for the AM1 calculated values as the larger oligomers are included in the determination. Figure 1 also shows the AM1 fit, using only the range of n used in the experimental determination, but Figure 2 shows the full range of available AM1 data with the fit from Figure 1 to show the poorness of the fit. This is because a is predicted by AM1 to be a function of n. The experimental data are not precise enough to determine if the actual relationship is truly linear.

Because most PDA derivatives tend to be insoluble, there are few experimental measurements of their optical properties. Thus for a relative assessment of the method, our AM1 calculated parameters are compared to values from previous work using ab initio (4-31G and STO-3G basis sets in GAUSSIAN 86) and semiempirical INDO methods,[19] shown in Figure 3. Although the AM1 values are substantially different from those of the 4-31G ab initio values, the trends are consistent, such that the ratio AM1/4-31G is 1.89 ± 0.03 for each pair of

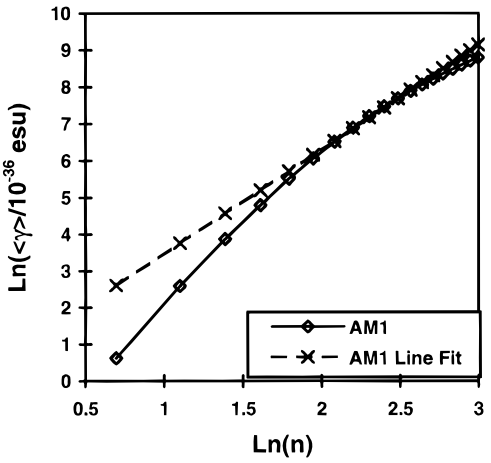

Figure 2. Plot of $\ln(\langle\gamma\rangle/10^{-36}$ esu) vs $\ln(n)$ for AM1 computed $\langle\gamma\rangle$ values of acetylene oligomers for $n = 2$ to $n = 20$, but with the best fit line for $n = 8-13$ (excluding 9).

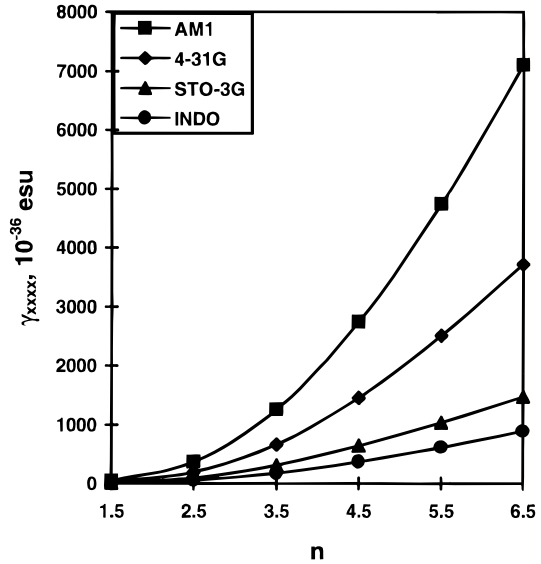

Figure 3. Comparison of γ_{xxxx} vs n trends for AM1 with previous calculations for PDA oligomers.

data points from $n = 1.5$ to $n = 6.5$. Thus, assuming that the deviations do not increase substantially, the comparison of the two sets of calculations should only require a simple scaling factor, as is also true to the INDO calculations, with INDO/4.31G = 0.20 ± 0.04.

Effect of Noncoplanarity on ODDO Properties. Calculations predict that rotation of one acetyl group relative to the plane containing the backbone and the other acetyl group leads to some change in the monomer's heat of formation, ΔH_f, and optical properties but negligible changes in bond lengths and angles. The structure of ODDO and poly-ODDO below shows the planar conformer with syn carbonyl groups ($\phi_1 = 0°$). The more stable planar conformer is the anti conformer ($\phi_1 = 180°$) and the most stable conformation is found at $\phi_1 \cong 110°$.

The change in the HOMO−LUMO gap E_g as a function of the dihedral angle ϕ_1 is shown in Figure 4. E_g for the most stable conformer is predicted to be 9.95 eV, which is 1.15 eV lower in energy than the calculated value of E_g for DA. The minimum E_g is 9.71 eV, which occurs at $\phi_1 = 180°$ increases until the two acetyl C═O bonds are perpendicular to each other ($\phi_1 = 90°$); the gap at that point is 0.38 eV greater than the minimum.

(18) Kurtz, H. A. *Int. J. Quantum Chem. Symp.* **1990**, *24*, 791.
(19) Kirtman, B.; Hasan, M. *Chem. Phys. Lett.* **1989**, *157*, 123.
(20) Koski, H. K. *Acta Crystallogr.* **1975**, *B31*, 933.

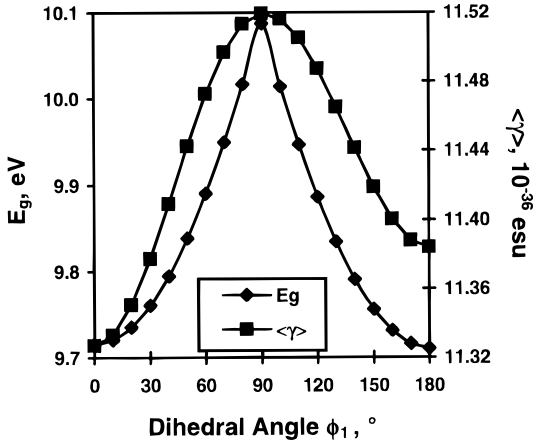

Figure 4. Plots of HOMO−LUMO gap E_g and second hyperpolarizability $\langle\gamma\rangle$ as a function of the dihedral angle ϕ_1 in Scheme 1.

These data suggest that the acetyl group has a more pronounced influence on the electronic energies of DA derivatives than the methyl or chlorine groups that we previously studied.[3] The mean second hyperpolarizability $\langle\gamma\rangle$ is also shown in Figure 4. It can be concluded from the figure that E_g is largest when the conjugation length is the smallest, which occurs when the two acetyl groups are perpendicular. However, $\langle\gamma\rangle$ is also the largest when the conjugation length of the monomer is the smallest. We propose that the increase is due to the fact that, although the overall conjugation length is smaller at $\phi_1 = 90°$ than $\phi_1 = 180°$, there are now two smaller perpendicular conjugation chains, due to the single-bond and the triple-bond alternation of the ODDO backbone, with each acetyl group contributing to a different conjugation chain.

Effect of Substituent Orientation on Poly-ODDO. As models for poly-ODDO, we have chosen oligomeric structures which incorporate two full monomer units plus end groups, each containing an acetyl group. This type of structure allows us to include the effects of hydrogen-bonding and steric effects between the central acetyl groups and their neighbors. In a previous article,[3] we demonstrated the relevance of oligomeric structures as models of PDA derivatives.

In the polymeric model, each acetyl group can have two different coplanar positions, one with the C═O bond almost parallel to the C≡C bond in the backbone, and the other with the C═O bond almost parallel to the C═C double bond. Since there are a total of six acetyl groups in our simple model, there are $2^6 = 64$ different coplanar conformers. We further assumed that the end units would be the same. In other words, the two leftmost acetyl groups would have the same orientation as the two rightmost acetyl groups (ABA repeat stereochemistry). This reduces the total conformers to $2^4 = 16$ conformers. Six conformers are related to another six by a 2-fold axis of rotation, leaving a total of ten conformers. These conformers are shown in Table 1. The ten model conformers of poly-ODDO are shown in order of decreasing stability as predicted by calculated values of ΔH_f. In addition, the dipole moment μ, HOMO−LUMO gap E_g, and mean second hyperpolarizability $\langle\gamma\rangle$ for the different planar structures of poly-ODDO are compiled in Table 1. Of the ten coplanar conformations, structure **1** is predicted to have the greatest relative stability. We see from the structures

Table 1. AM1 Calculated Properties for ODDO Polymer Model Structures

ΔH_f (kcal/mol)	μ (Debye)	E_g (eV)	$\langle\gamma\rangle$ (10^{-36} esu)	ΔH_f (kcal/mol)	μ (Debye)	E_g (eV)	$\langle\gamma\rangle$ (10^{-36} esu)
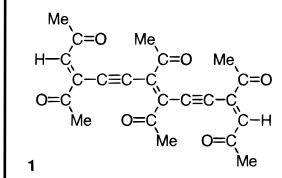 **1**				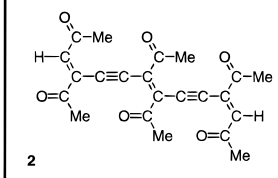 **2**			
-57.7	0.0	7.46	101	-48.8	14.5	7.35	110
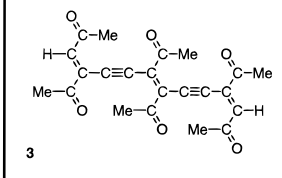 **3**				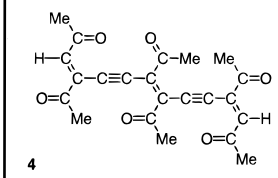 **4**			
-43.4	0.0	7.52	100	-43.1	4.4	7.43	102
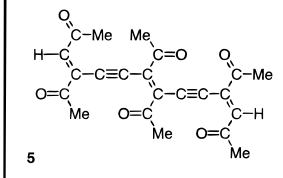 **5**				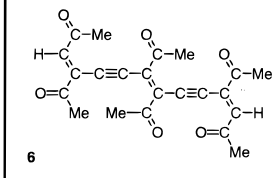 **6**			
-42.1	9.9	7.45	105	-35.5	10.2	7.51	107
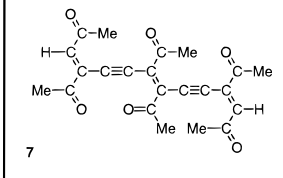 **7**				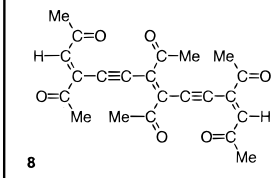 **8**			
-35.4	4.6	7.41	110	-31.6	0.0	7.55	92
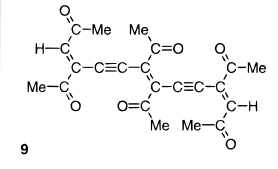 **9**				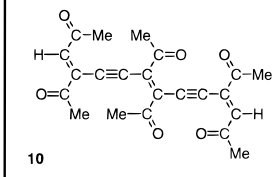 **10**			
-30.1	0.0	7.46	107	-26.1	5.6	7.47	103

Table 2. AM1 Computed O···H Distances and C═O···H Angles for the Model Compounds in Table 1

model	quantity	O···H distance (Å)	C−H···O angle (deg)
1	8	2.21	101
2	4	2.21−2.22	101
	4	2.30	92−93
3	8	2.30−2.31	92−93
4	4	2.19−2.25	101−102
5	4	2.19−2.23	101−102
6	4	2.28−2.34	91−93
7	4	2.27−2.33	92

in Table 1 that the three most stable structures have maximum hydrogen-bonding interaction (eight bonds), the next four most stable structures have moderate hydrogen-bonding interaction (four bonds), and the three least stable structures have no hydrogen-bonding interaction. The hydrogen-bond interaction angles and distances are shown in Table 2, with the shortest distances being equivalent to standard AM1 computed hydrogen-bond lengths.[13] We therefore assume that hydrogen bonding plays the largest part in determining the structure's relative conformational stability among

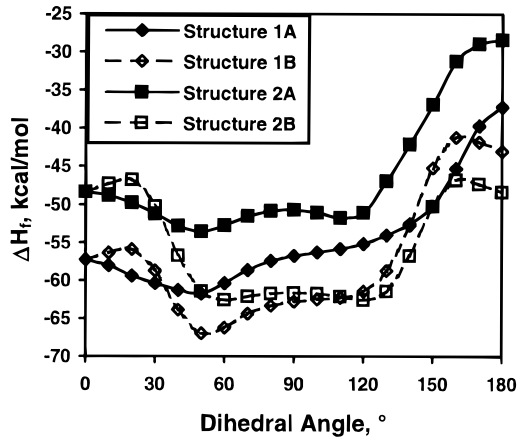

Figure 5. Plots of heat of formation ΔH_f as a function of the dihedral angle rotation for the backbone of structure **1**, ϕ_2 in structure **1A**, the acetyl group substituent of structure **1**, ϕ_3 in structure **1B**, the backbone of structure **2**, ϕ_4 in structure **2A**, the acetyl group substituent of structure **2**, ϕ_5 in structure **2B**.

possible coplanar conformations. Second, the ΔH_f for the structures appears to be affected by steric interactions between the methyl groups and the backbone, with the most stable structures being those that have the methyl groups in lowest proximity to the backbone. Since these structures model long chain polymers, three of the structures become the same as three others as more repeat units are added (i.e., ABA ⇔ BAB): **4** ≡ **5**, **6** ≡ **7**, and **8** ≡ **9**. We would then expect the polymer's relative stability to the other polymers being modeled to be proportional to the average of each pair. One would also expect E_g and $\langle\gamma\rangle$ to converge for each pair.

Data from Table 1 indicate that stability is highly dependent on conformation. E_g varies only as much as 0.2 eV among the models, and $\langle\gamma\rangle$ varies less than 20% among the models, with less than 10% between the two most stable conformers. This suggests attempts to control the substituent orientation would not be very productive for maximizing optical properties. It should also be noted that the order of decreasing E_g does not always correspond to increasing $\langle\gamma\rangle$, so E_g may not always be a good indicator of $\langle\gamma\rangle$ behavior for different conformers.

Effect of Nonplanarity on Poly-ODDO. Crystallization of diacetylene monomers often leads to crystalline polymers with slight nonplanarity of the backbone and with pendant groups positioned for minimum nonbonding interactions or for maximum through-space interactions (e.g., hydrogen bonding). Thus we chose to use poly-ODDO as a model to investigate stability, electronic, and optical properties, which were predicted as a function of nonplanarity of the backbone and the acetyl groups. The two most stable models from Table 1 were used for backbone rotation and acetyl group rotation, because the second most stable model is predicted to have the best optical properties. Structure **1A** shows the direction of backbone dihedral angle rotation ϕ_2 for structure **1**, structure **1B** shows the direction of rotation of acetyl group dihedral angle rotation ϕ_3 for structure **1**, and structures **2A** and **2B** show the equivalent rotations ϕ_4 and ϕ_5 for structure **2**. 0° represents the original planar model in each case.

Figure 5 shows the effect of nonplanarity on stability. For structures **1A** and **2A**, in which the acetyl groups

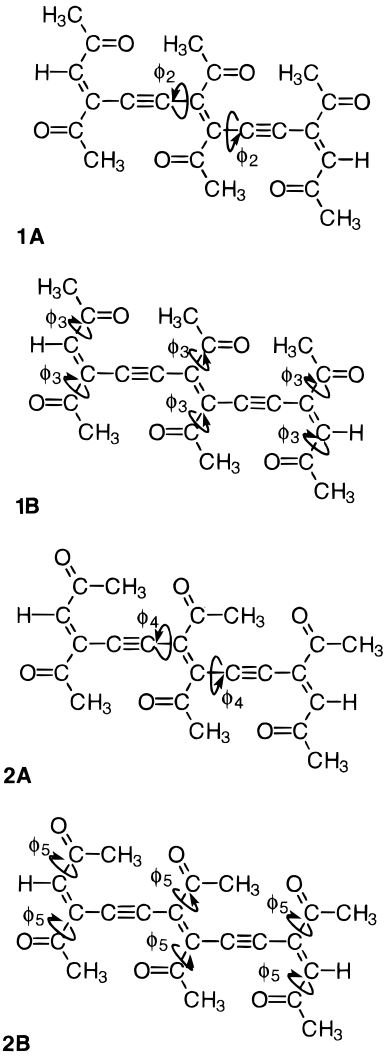

are fixed to remain planar with the double bond to which they are attached, the models are predicted to be 4.4 and 5.2 kcal/mol more stable at the global minima of 50°, respectively, than the initial planar conformations (0°). For structures **1B** and **2B**, in which the backbone dihedral angles are fixed to remain planar, the models are predicted to be 9.7 and 14.2 kcal/mol more stable at the global minima of 50° and 60°, respectively, than the initial coplanar conformations. Note that for acetyl group rotation, structure **1B** at 180° is equivalent to structure **3** from Table 1, while structure **2B** at 180° is equivalent to itself at 0°. The data indicate that completely coplanar structures are unlikely to be formed and that steric factors overcome any hydrogen-bonding interactions between adjacent acetyl groups, but that substituent deformation is thermodynamically preferable to backbone deformation. In fact, calculations which allow both ϕ_2 and ϕ_3 to simultaneously minimize for structure **1** confirm this, and predict that the most stable conformers are at $\phi_2 = 0°$ and $\phi_3 = 50°$.

Figure 6 shows the effect of nonplanarity on E_g. For structures **1A** and **2A**, the models are predicted to have 0.69 and 0.74 eV larger E_g at the global maxima of 90°, respectively, than the initial planar conformations (0°), which are the global minima. For structures **1B** and **2B**, the models are predicted to have 0.47 and 0.57 eV larger E_g at the global maxima of 90°, respectively, than the initial planar conformations (0°), which are the

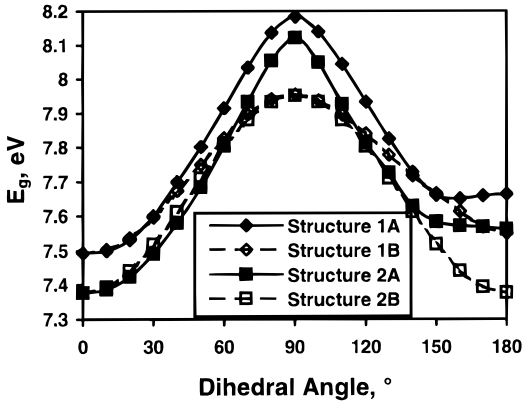

Figure 6. Plots of the HOMO−LUMO gap E_g as a function of the dihedral angle rotation for the backbone of structure **1**, ϕ_2 in structure **1A**, the acetyl group substituent of structure **1**, ϕ_3 in structure **1B**, the backbone of structure **2**, ϕ_4 in structure **2A**, the acetyl group substituent of structure **2**, ϕ_5 in structure **2B**.

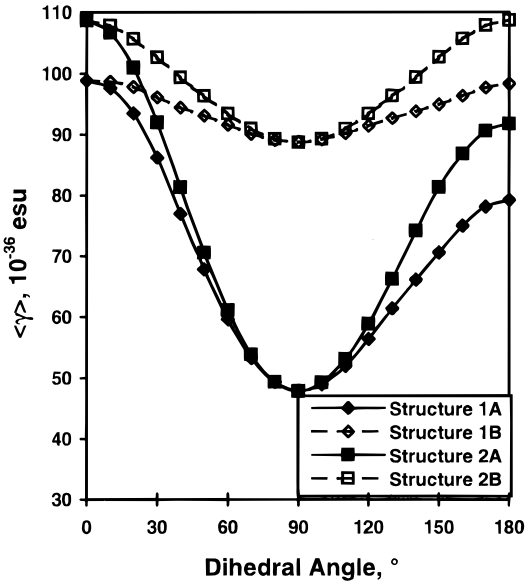

Figure 7. Plots of the mean second hyperpolarizability $\langle\gamma\rangle$ as a function of the dihedral angle rotation for the backbone of structure **1**, ϕ_2 in structure **1A**, the acetyl group substituent of structure **1**, ϕ_3 in structure **1B**, the backbone of structure **2**, ϕ_4 in structure **2A**, the acetyl group substituent of structure **2**, ϕ_5 in structure **2B**.

global minima. The data indicate that completely planar structures have the lowest values for E_g, while those with the greatest nonplanarity (90°) have the highest values for E_g. This is as expected. Furthermore, backbone nonplanarity is nearly twice as effective in raising E_g as acetyl group noncoplanarity. One would expect this effect to be even greater for longer chain length models.

Figure 7 shows the effect of nonplanarity on $\langle\gamma\rangle$. For structures **1A** and **2A**, the models are predicted to have 52% and 56% smaller $\langle\gamma\rangle$ at the global minima of 90°, respectively, than the initial planar conformations (0°), which are global maxima. For structures **C** and **E**, the models are predicted to have 10% and 20% smaller $\langle\gamma\rangle$ at the global minima of 90°, respectively, than the initial planar conformations (0°), which are the global maxima. The data indicate that completely planar structures have the highest values for $\langle\gamma\rangle$, while those with the greatest nonplanarity (90°) have the lowest values for $\langle\gamma\rangle$. Furthermore, backbone nonplanarity is nearly 3−5

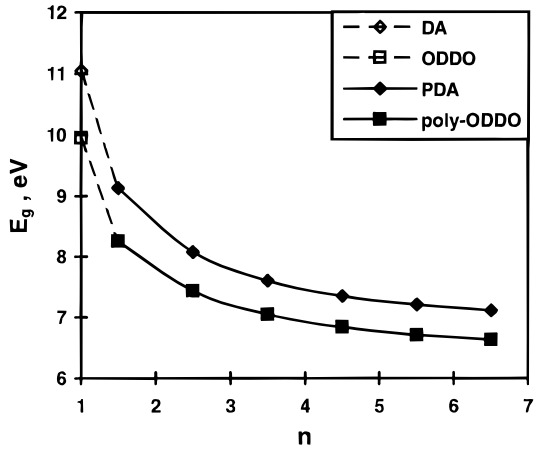

Figure 8. Plot of AM1 calculated HOMO−LUMO gap E_g vs n for the monomers (n = 1) of DA (Scheme 1, R = H) and ODDO (Scheme 2) and several oligomers (n > 1) of PDA (structure **11**, R = H) and the most stable ODDO conformer (structure **12**).

times as important in lowering $\langle\gamma\rangle$ than is acetyl group noncoplanarity. One would expect this difference to be even greater for longer chain length models.

Effect of Conjugation Length on the Electronic and Optical Properties of Poly-ODDO. Optical properties of poly-ODDO were calculated for several oligomers based on the three most stable coplanar poly-ODDO structures from Table 1. The trends for unsubstituted diacetylene oligomers, structure **11**, with R = H, are shown in relation to that oligomeric poly-ODDO structure, structure **12**, for E_g and $\langle\gamma\rangle$ as a function of the poly-ODDO model size n in Figures 8 and 9, respectively. Figure 10 also shows the plot of $\ln(E_g)$ vs $\ln(\langle\gamma\rangle)$ for the same model structures.

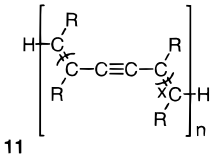

11

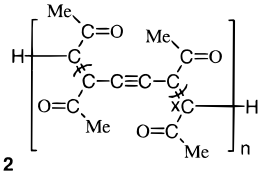

12

It can be seen from Figures 8 and 9 that the trends between unsubstituted diacetylene oligomers and the ODDO oligomers are similar, with E_g for each ODDO oligomer being within 1 eV lower than the corresponding unsubstituted oligomer and with the two curves apparently converging very slightly. All three of the most stable ODDO structures give essentially the same curve for E_g. $\langle\gamma\rangle$ is also seen to have similar trends between the two curves, with the ODDO oligomer $\langle\gamma\rangle$ values increasing at a greater rate than the unsubstituted oligomer $\langle\gamma\rangle$ values, as would be expected. Again, the two most stable poly-ODDO model structures have nearly the same curve, but $\langle\gamma\rangle$ for structure **2** oligomers increases at a slighter faster rate. Finally, Figure 10 shows that it is unwise to use the AM1 computed monomer values to predict polymeric optical property trends, as seen from the crossover in the curves. It may

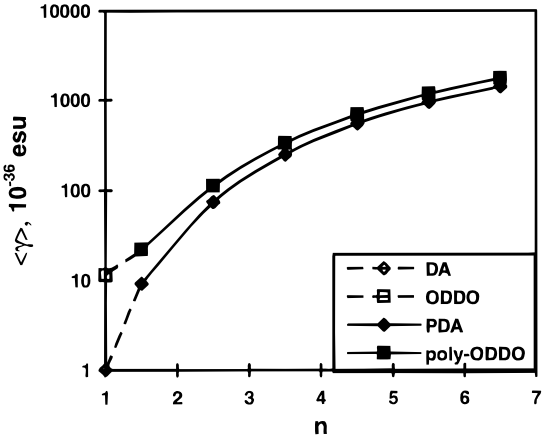

Figure 9. Plot of AM1 calculated second hyperpolarizability $\langle\gamma\rangle$ vs n for the monomers (n = 1) of DA (Scheme 1, R = H) and ODDO (Scheme 2) and several oligomers (n > 1) of PDA (structure **11**, R = H) and the most stable ODDO conformer (structure **12**).

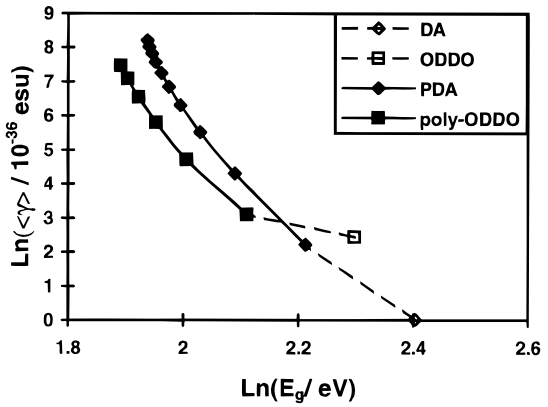

Figure 10. Plot of AM1 calculated natural log of HOMO−LUMO gap, ln(E_g), vs the natural log of the mean second hyperpolarizability, ln($\langle\gamma\rangle/10^{-36}$ esu), for the monomers (n = 1) of DA (Scheme 1, R = H) and ODDO (Scheme 2) and several oligomers (n > 1) of PDA (structure **11**, R = H) and the most stable ODDO conformer (structure **12**).

also be unwise to try to use E_g from DA and its derivatives to predict optical properties, since a given value for E_g for DA and its derivatives may not map to the same $\langle\gamma\rangle$. ODDO has substituents which effectively extend the conjugation length beyond that of DA. In poly-ODDO, these substituents play a different role, in that they do not provide extension of the backbone conjugation but rather provide conjugation in a perpendicular axis. As the oligomer size increases, their role in the overall $\langle\gamma\rangle$ decreases. The substituent conjugation is responsible for the offset between the two curves in Figure 10 and may not be adequately accounted for by the free-electron model that relates E_g to $\chi^{(3)}_{xxxx}$, which is in turn proportional to $\langle\gamma\rangle$ for one-dimensional molecules like PDA and its derivatives.[1c]

With regard to the degree of perpendicular conjugation (γ_{yyyy}) and cross-conjugation (γ_{xxyy}) in poly-ODDO models, the poly-ODDO model structure with n = 1.5 is predicted to have a contribution from γ_{yyyy} that is 26.7% of γ_{xxxx} and a contribution from γ_{xxyy} that is 3.3% of γ_{xxxx}. By the time n = 6.5, the contribution from γ_{yyyy} has fallen to 0.7% of γ_{xxxx} and a contribution of γ_{xxyy} has fallen to 0.5% of γ_{xxxx}. This tends to suggest that the primary optical property advantage of the acetyl group is to enhance the backbone conjugation and corresponding γ_{xxxx}.

Monomer Reactivity. It has been noted that ODDO undergoes rapid reaction when solvent is removed from a dilute solution of the monomer. A gas-phase study was made using AM1 to determine the importance of thermodynamics in this reaction. Heats of formation, ΔH_f, and entropies, S, were computed for several derivatives of DA and PDA, including ODDO and poly-ODDO. These properties are related to ΔG_f by $\Delta G_f = \Delta H_f - T\Delta S_f$, where T is standard temperature (298 K) in all cases. Due to the nature of the computations, as discussed previously, only relative values should be considered. In this case, one should use $\Delta G = (\Delta H - TS)_2 - (\Delta H - TS)_1$.[12,16] This equation also cancels the unknown values of the computed entropies of formation, ΔS_f, of the constituent elements.

The results of the calculations are shown in Table 3. The monomer model is shown in Scheme 1, and the oligomer model is shown in structure **11**. ΔH_f(m) is the heat of formation of the monomer. $\Delta\Delta H_f$(o) = ΔH_f-(n=2.5) − ΔH_f(n=1.5) is the difference in heats of formation between the two oligomers and represents the heat of formation of a monomeric unit. $\Delta\Delta\Delta H_f = \Delta H_f$-(m) − $\Delta\Delta H_f$(o) is the difference between the monomer heat of formation, ΔH_f(m), and the monomeric unit heat of formation in an oligomer, $\Delta\Delta H_f$(o), so higher values indicate a greater stability of the monomeric unit relative to the monomer. Calculations for some oligomers with n = 3.5 indicate that there is very little change in $\Delta\Delta H_f$(o) as one goes to larger oligomers, as one would expect. For entropy, S(m) is the entropy of the monomer. ΔS(o) = S(n=2.5) − S(n=1.5) is the difference in entropies between the two oligomers and represents the entropy of a monomeric unit. $\Delta\Delta S$ = S(m) − ΔS(o) is the difference between the monomer entropy, S(m), and the monomeric unit entropy in the oligomer, ΔS(o), so higher values indicate a lower entropy of the monomeric unit relative to the monomer. $\Delta\Delta\Delta G = \Delta\Delta\Delta H_f - T\Delta\Delta S$ (where T = 298 K) is the difference in free energies of formation for the monomer and the monomeric unit. Higher values of $\Delta\Delta\Delta G$ indicate greater stability of the monomeric unit in the oligomer (i.e., free energy change of going from the monomer to the monomeric unit in an oligomer would be negative).

Table 3. Monomeric Unit vs Monomer Stability Heats of Formation (kcal/mol), Entropies (cal/mol/K), and Free Energies for Derivatives (kcal/mol) of DA and PDA, as Well as Activation Energies (kcal/mol) between Monomer Ground-State and Diradical Excited-State Monomer Model Shown in Scheme 1 and the Oligomeric Model Shown in Structure 11

R = (ref)	ΔH_f (m)	$\Delta\Delta H_f$(o)	$\Delta\Delta\Delta H_f$	S(m)	ΔS(o)	$\Delta\Delta S$	$\Delta\Delta\Delta G$	E_a
−H (20)	106.08	63.95	42.13	57.79	25.82	31.97	32.60	91.52
$-CH_2CH_2OH$ (21)	−22.22	−53.13	30.91	113.04	68.52	44.52	17.64	82.51
−phenyl (22)	148.65	122.49	26.16	116.70	74.57	42.13	13.61	104.35
−tosylate (23)	−87.12	−124.11	36.99	194.59	131.23	63.36	18.11	95.50
$-C(O)CH_3$ (7)	30.30	−3.31	33.61	107.19	56.97	50.22	18.64	75.35
−ketal (7)	−67.89	−96.70	28.81	133.35	74.50	58.85	11.27	85.74

Neglecting the unsubstituted case, one sees that $\Delta\Delta\Delta G$ values for the poly-ODDO and the diol (R = $-CH_2CH_2OH$) are the largest and that those series should be the most reactive on thermodynamic grounds alone, assuming similar reaction mechanisms for all DA and PDA derivatives. However, the $\Delta\Delta\Delta H_f$ values are highest for the ditosylate, indicating the greatest stability gain of the series for polymerization. The diphenyl and diketal series are predicted to have the lowest stability and free energy gains upon polymerization. The unsubstituted monomer is predicted to react most favorably toward polymerization. Experimentally, it is known that the diol monomer is reactive in the solid state[21] and that the ditosylate is known to react over time in the solid state even in the dark.[23] Both the diphenyl and diketal series are relatively stable to polymerization.[22,24] Unsubstituted DA is a gas and has not been studied in solution or solid state where close contact of monomer units allow verification of the monomer's reactivity at standard temperature.[20] Thermodynamics does not appear to play the major role in solid-state reactions, and its role in photopolymerization in solution is not yet clear.[24] It is nonetheless interesting that the gas-phase trends predict reactivity for known reactive DA derivatives that are similar to experimental results in the solid state. Monomer excited states (diradicals) were also computed for each of the derivatives to see if some further insight might be gained into the high reactivity of ODDO. This information is also included in Table 3 as E_a, which is the difference between the monomer excited-state and ground-state heats of formation. It is interesting to note that ODDO has the lowest computed E_a.

The substantial reactivity of ODDO is not indicated by the results, though it is predicted to be one of the more reactive monomers. This may either be a result of the fact that thermodynamic gas-phase calculations may not adequately incorporate the factors involved in liquid- or solid-state polymerization, as one might suspect for reactions in which excited states play a major part, or that MOPAC may not be suitable to making qualitative statements involving some thermodynamic properties for DA derivatives.

Acknowledgment. Financial support by the National Aeronautics and Space Administration (Contract NAGW-812) and the NASA Space Grant Fellowship Program is gratefully acknowledged.

CM950451W

(21) Fisher, D. A.; Ando, D. J.; Batchelder, D. N.; Hursthouse, M. B. *Acta Crystallogr.* **1978**, *B34*, 3799.
(22) Wiebenga, E. H. *Z. Kristallogr.* **1940**, *102*, 193.
(23) Kobelt, V. D.; Paulus, E. F. *Acta Crystallogr.* **1974**, *B30*, 232.
(24) Paley, M. S.; Frazier, D. O.; Abdeldeyem, H.; Armstrong, S.; McManus, S. P. *J. Am. Chem. Soc.* **1995**, *117*, 4775.